ENVIRONMENTAL RESEARCH
LETTERS

CrossMark

LETTER

Chronically underestimated: a reassessment of US heat waves using the extended heat index

David M Romps[1,2,*] and Yi-Chuan Lu[2,3]

[1] Department of Earth and Planetary Science, University of California, Berkeley, CA, United States of America
[2] Climate and Ecosystem Sciences Division, Lawrence Berkeley National Laboratory, Berkeley, CA, United States of America
[3] Department of Physics, University of California, Berkeley, CA, United States of America
[*] Author to whom any correspondence should be addressed.

E-mail: romps@berkeley.edu

Abstract

The heat index, or apparent temperature, was never defined for extreme heat and humidity, leading to the widespread adoption of a polynomial extrapolation designed by the United States National Weather Service. Recently, however, the heat index has been extended to all combinations of temperature and humidity, presenting an opportunity to reassess past heat waves. Here, three-hourly temperature and humidity are used to evaluate the extended heat index over the contiguous United States during the years 1984–2020. It is found that the 99.9th percentile of the daily maximum heat index is highest over the Midwest. Identifying and ranking heat waves by the spatially integrated exceedance of that percentile, the Midwest once again stands out as home to the most extreme heat waves, including the top-ranked July 2011 and July 1995 heat waves. The extended heat index can also be used to evaluate the physiological stress induced by heat and humidity. It is found that the most extreme Midwest heat waves tax the cardiovascular system with a skin blood flow that is elevated severalfold, approaching the physiological limit. These effects are not captured by the National Weather Service's polynomial extrapolation, which also underestimates the heat index by as much as $10\,°C$ ($20\,°F$) during severe heat waves.

1. Introduction

Among meteorological phenomena, heat waves are the number one cause of death in the United States (Changnon *et al* 1996). Heat waves pose a particular threat to the elderly (Carleton *et al* 2020), those without access to air conditioning (O'Neill *et al* 2005), and outdoors workers (Acharya *et al* 2018). As the Earth warms, the frequency and severity of heat waves is expected to increase (Dosio *et al* 2018). It is important, therefore, to have accurate metrics for heat waves, both to issue operational warnings and to plan adaptations for the future.

Many different metrics have been used to define, identify, and measure heat waves (Xu *et al* 2016). Defined as having an anomalously high air temperature, heat waves in the contiguous United States (CONUS) are found to be most severe in the South (Meehl and Tebaldi 2004, Dosio *et al* 2018). Heat

waves have also been defined using the heat index, also known as the apparent temperature, which is a metric that maps one-to-one onto physiological states (different rates of skin blood flow) in hot conditions (Steadman 1979). Most studies that define heat waves in terms of the heat index also find that the frequency of heat waves peaks in the South (e.g. Smith *et al* 2013, Lyon and Barnston 2017). An exception is the study of Robinson (2001), who found that heat waves are comparably frequent in the South, Midwest, and Mid-Atlantic.

It is notable, however, that these studies—and all other studies that have used Steadman's heat index to study heat waves—have used not the actual heat index, but a functional approximation to the heat index. Of the many different approximations (Anderson *et al* 2013), the most widely used is the polynomial fit developed by the United States National Weather Service (Rothfusz 1990, National

Weather Service 2014). The National Weather Service (NWS) approximation is used on a regular basis to issue warnings to the public and to study past severe heat (e.g. Robinson 2001, Kim *et al* 2006, Yip *et al* 2008, Smith *et al* 2013, Lyon and Barnston 2017, Tustin *et al* 2018, Xie *et al* 2018, Perera *et al* 2022) and future severe heat (e.g. Delworth *et al* 1999, Diffenbaugh *et al* 2007, Opitz-Stapleton *et al* 2016, Diem *et al* 2017, Modarres *et al* 2018, Dahl *et al* 2019, Rao *et al* 2020, Rahman *et al* 2021, Amnuaylojaroen *et al* 2022). Even in the current climate, there are conditions hotter and more humid than were considered and tabulated by Steadman (1979), and so the NWS approximation is used to extrapolate the heat index beyond those tabulated values. That extrapolation is used extensively in operational warnings and in the aforementioned research studies.

From the perspective of social impacts, heat waves would ideally be identified and quantified using not an extrapolation but an accurate measure of physiological stress. Recently, Lu and Romps (2022) extended Steadman's heat index to all combinations of temperature and humidity, providing such a measure. The objectives of this paper are threefold: (a) to use the extended heat index to define and rank the most severe heat waves experienced over the United States during recent decades, (b) to evaluate the extent to which the NWS approximation errs in reporting the heat index during those heat waves, and (c) to evaluate the physiological state required of humans exposed to conditions during the most severe of those heat waves.

2. The heat index

To motivate the use of the heat index, we give here a brief review. As is well known, sweating is a physiological adaptation to high temperatures, with the evaporation of sweat providing a cooling effect. But this adaptation has limits: if the air is sufficiently hot and humid, evaporative cooling is unable to compensate for the inputs of metabolic heat, sensible heat, and infrared radiation, and the core temperature rises. In general, in hot and humid conditions, humans are subjected to greater physiological stress if either the temperature or humidity increases.
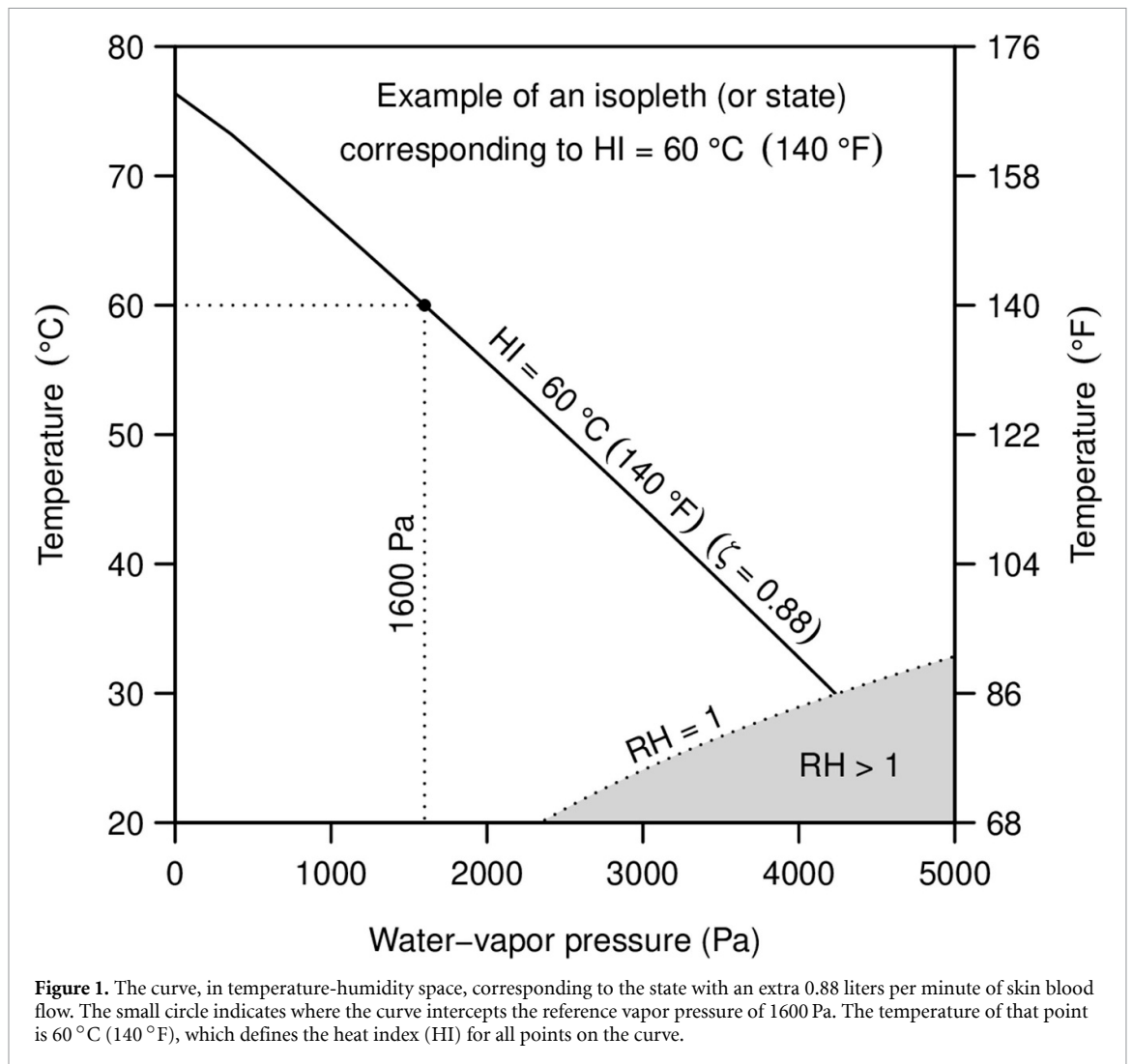
To capture these effects, Steadman (1979) developed a model of thermoregulation with parameters chosen to represent a healthy adult walking in the shade with ample access to drinking water. The model quantifies the behavior (clothing thickness) and physiology (skin blood flow) in response to a combination of temperature and humidity. An important aspect of this model is that the human responds to changes in temperature and humidity by adjusting only one parameter at a time. For example, in relatively cold conditions, the human responds to changes in temperature by adjusting the thickness of

the clothing being worn. Once that response has been exhausted (i.e. the clothing thickness has been driven to zero), the human responds by adjusting its skin blood flow. As a consequence, all states form a one-dimensional family, i.e. the states can be parameterized by a single variable. For example, in the original Steadman model, the states could be parameterized by ζ with the clothing thickness in millimeteres equal to $-\zeta$ for $\zeta < 0$ and the skin blood flow, in liters per minute, elevated by an amount of ζ for $\zeta \geqslant 0$.

Since the space of states is one-dimensional, whereas the space of all possible temperature and humidity is two-dimensional, each state corresponds to a one-dimensional isopleth in temperature-humidity space. For example, all pairs of temperature and humidity corresponding to a clothing thickness of five millimeters form a continuous one-dimensional curve with $\zeta = -5$. So long as the actual air temperature and humidity remain on an isopleth, a human's experience of those conditions does not change (e.g. the choice of clothing or the skin blood flow remains the same). The heat index, which is a function of temperature and humidity, is simply a convention for assigning a unique temperature to each isopleth: the heat index is defined to be the temperature of the isopleth at 1600 Pa (Steadman 1979).

For illustration, figure 1 shows the curve corresponding to $\zeta = 0.88$ (the state with an extra $0.88\,\mathrm{l\,min^{-1}}$ of skin blood flow), which intercepts a vapor pressure of 1600 Pa at a temperature of $60\,^{\circ}\mathrm{C}$ ($140\,^{\circ}\mathrm{F}$). All pairs of temperature and humidity lying on this curve have a heat index of $60\,^{\circ}\mathrm{C}$ and induce identical behavioral and physiological responses (minimization of clothing and an extra skin blood flow of $0.88\,\mathrm{l\,min^{-1}}$). In this way, every pair of temperature and humidity can be mapped to a value of the heat index and a thermoregulatory state. This is useful for communicating the hazard posed by high heat and humidity. For example, a heat index of $60\,^{\circ}\mathrm{C}$ ($140\,^{\circ}\mathrm{F}$) corresponds to a skin blood flow that is about two and a half times its value at room temperature. Maintaining a high skin blood flow can stress the cardiovascular system, even leading to death by heart failure. On the other hand, failing to maintain the required skin blood flow would lead to an elevated core temperature, which, if elevated by only a few degrees, can lead to death by hyperthermia.

Unfortunately, the heat index defined by Steadman (1979) was defined only up to certain combinations of heat and humidity, beyond which the heat index was undefined. Those originally undefined regions are labeled V and VI in figure 8 of Lu and Romps (2022). For example, Steadman was unable to define the heat index for $30\,^{\circ}\mathrm{C}$ ($86\,^{\circ}\mathrm{F}$) at 90% relative humidity, or for $35\,^{\circ}\mathrm{C}$ ($95\,^{\circ}\mathrm{F}$) at 65% relative humidity. The heat index was left undefined in those conditions due to an apparent failure of the underlying model of thermoregulation: the vapor pressure

Figure 1. The curve, in temperature-humidity space, corresponding to the state with an extra 0.88 liters per minute of skin blood flow. The small circle indicates where the curve intercepts the reference vapor pressure of 1600 Pa. The temperature of that point is 60 °C (140 °F), which defines the heat index (HI) for all points on the curve.
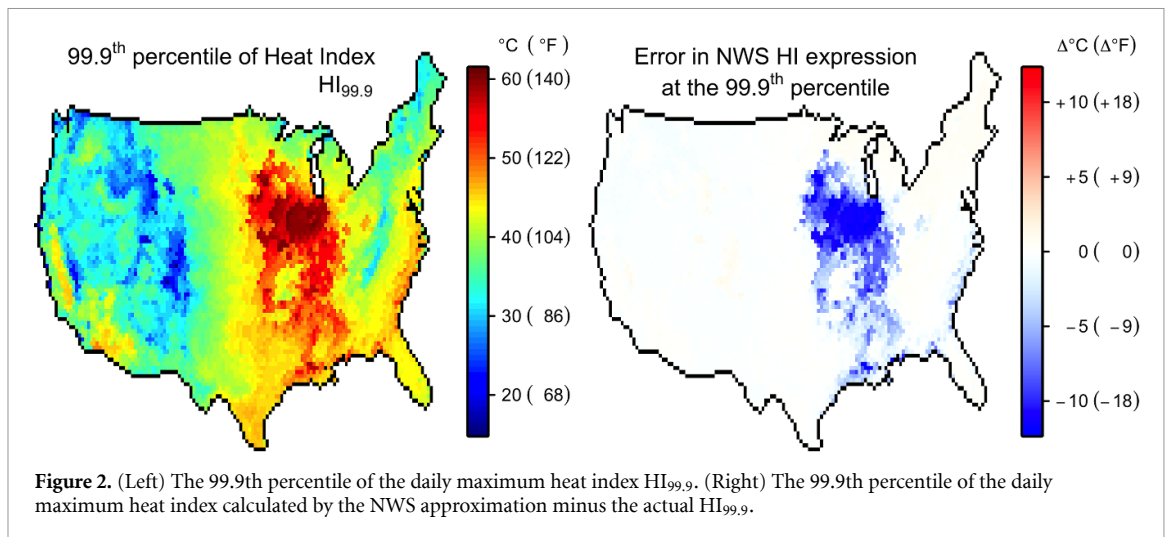
at the skin surface exceeded the saturation value. To allow for extrapolation beyond this point of apparent failure, the NWS developed and adopted a polynomial fit to the heat index as a function of temperature and humidity (Rothfusz 1990, National Weather Service 2014). But without a model of thermoregulation at the high values of temperature and humidity, those extrapolated values have no interpretation with respect to a thermoregulatory state. Furthermore, as will be shown below, the extrapolated values used by the NWS are biased low by ~10 °C (~20 °F) during the peaks of severe heat waves.

Recently, Lu and Romps (2022) showed that Steadman's model, and therefore the heat index, could be extended in a physical way. One of the keys to extending the model to high heat and humidity is to allow sweat to drip off the skin; this simple fix avoids any water-vapor supersaturation. This extension is backwards compatible—it gives the same values as the model of Steadman (1979) where the original model was defined—but extends the definition of the heat index to all combinations of temperature and humidity. And, as with the original heat index, every value maps one-to-one to a one-dimensional family of thermoregulatory states, which are parameterized by the fraction of skin covered by clothing in very cold conditions, the thickness of clothing in cold-to-mild conditions, the skin blood flow in hot conditions, and the rate of core-temperature rise in dangerously hot or lethal conditions.

3. Methods

To calculate the heat index (HI), we use the instantaneous two-meter temperature and humidity from the National Centers for Environmental Prediction (NCEP) North American Regional Reanalysis (NARR; Mesinger *et al* 2006), which provides data at a grid spacing of 32 km every three hours. We calculate the extended heat index (Lu and Romps 2022) for each three hourly snapshot from 1 January 1984 to 31 December 2020. We also calculate the polynomial fit to the heat index developed by the National Weather Service (Rothfusz 1990, National Weather Service 2014) with one minor modification made here to avoid bad behavior at cold temperatures (see the appendix).

Figure 2. (Left) The 99.9th percentile of the daily maximum heat index $HI_{99.9}$. (Right) The 99.9th percentile of the daily maximum heat index calculated by the NWS approximation minus the actual $HI_{99.9}$.

We will identify and quantify heat waves using the spatially integrated exceedance of the daily maximum heat index beyond its local 99.9th percentile of daily maxima. This choice defines heat waves in terms of their severity as perceived by humans, although there are other choices that could be made (e.g. weighting the exceedance by population density). The 99.9th percentile is chosen to isolate the most extreme events, i.e. those events comprised of values with a ~3 year (1000 day) return period.

We first define a grid cell's daily maximum heat index HI_{dm} as the highest HI among UTC 12, 15, 18, and 21 on the same date and UTC 0, 3, 6, and 9 of the following day. During spring, summer, and early fall, when CONUS is observing daylight saving, this captures all available NARR data from 5am to 2am (next day) local time on the West Coast and 8am to 5am (next day) local time on the East Coast. With 37 years of data, this gives 13 515 daily maximum values. The next step is to calculate, separately for each grid cell, the 99.9th percentile of HI_{dm} over all 13 515 days, which we denote by $HI_{99.9}$.

The map of $HI_{99.9}$ is shown in the left panel of figure 2. We see that the most extreme values of the heat index do not occur in the South as one might expect, but in the Midwestern states of Illinois, Iowa, and Missouri. In those states, the 99.9th percentile of the daily maximum heat index reaches up to and beyond 60 °C (140 °F). As seen in the right panel of figure 2, these extreme values are not captured by the polynomial extrapolation used by the NWS. In those midwestern states, the 99.9th percentile is underestimated by the NWS polynomial by as much as ~10 °C (~20 °F).
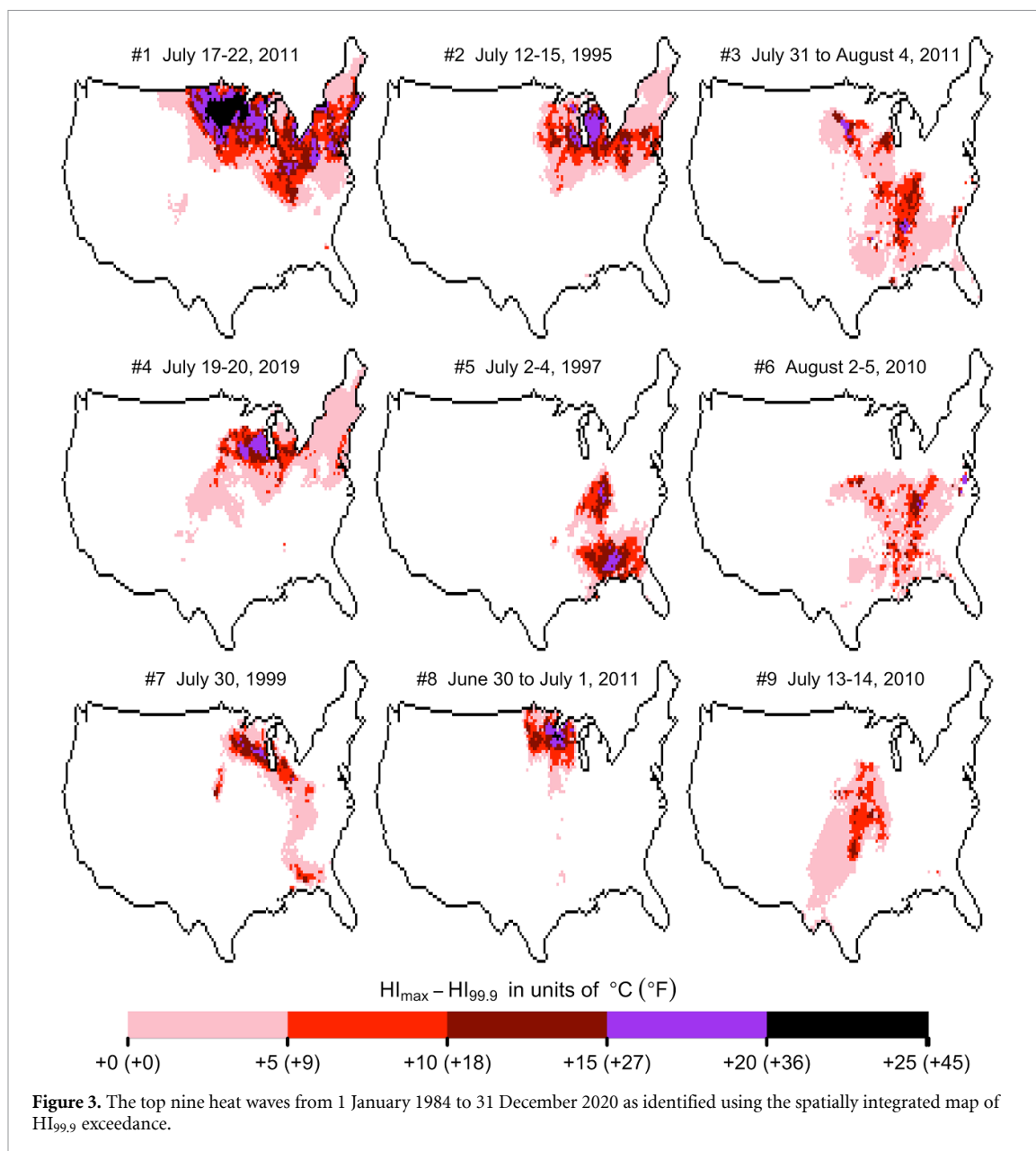
To prepare to identify heat waves, we first calculate the daily time series of the integral over CONUS of the number of degrees that HI_{dm} is in excess of the 99.9th percentile,

$$\int_{CONUS} dx\, dy \max\left[0, HI_{dm}(x,y,d) - HI_{99.9}(x,y)\right],$$

where x and y denote east–west and north–south distance and d denotes the day. This time series has 13 515 values: one for each day from 1 January 1984 to 31 December 2020. To find the first heat wave, we identify the maximum value in this time series. To find the start and end of that heat wave, we find the largest contiguous interval in that time series containing that maximum for which all values are at least 25% as large as that maximum; this defines the heat wave. We then find the two nearest local minima that bracket that heat wave and set to zero the interval that starts and ends with those two local minima. We then repeat the process to find the second heat wave, and so on. This identifies heat waves naturally ranked by the peak of their area-integrated exceedance of $HI_{99.9}$. The sensitivity of this ranking to the threshold, chosen here to be 25%, is explored in figures S1 and S2. A lower threshold would result in longer-duration heat waves, but would not substantially alter the ranking of the most severe heat waves: for threshold values ranging from 4% to 34%, the ranking of the top five heat waves is unchanged.

4. Results

For visualization of a heat wave, we define HI_{max} for each grid cell as the largest HI_{dm} in that grid cell during the days of the heat wave. For each of the top nine heat waves identified by the algorithm described above, figure 3 displays HI_{max} minus $HI_{99.9}$. The most severe heat wave (heat wave #1) is found to be centered on the Midwest during 17–22 July 2011. This time and place corresponds to a heat wave that generated a raft of news coverage and a dramatic spike in heat-related illness (Storm and Fowler 2011, Berry *et al* 2013, Fuhrmann *et al* 2016). The second most severe heat wave (heat wave #2) is identified as occurring over the same region during 12–15 July 1995. This again corresponds to a well-known heat wave that hit the city of Chicago especially hard, leading to hundreds of heat-related deaths (Semenza *et al* 1996,

Figure 3. The top nine heat waves from 1 January 1984 to 31 December 2020 as identified using the spatially integrated map of $HI_{99.9}$ exceedance.

1999, Whitman *et al* 1997, Dematte *et al* 1998). A list of the top 20 heat waves is given in table 1. Although the Midwest occupies only 26% of the area of the contiguous United States, it contains the peak heat index during 7 of the top 10 heat waves. This is particularly notable in comparison to the South, which occupies 29% of the area, but contains the peak heat index during only 3 of the top 10 heat waves. A list of the top 100 heat waves identified by this algorithm is given in tables S1 and S2 and maps of their $HI_{max} - HI_{99.9}$ are shown in figure S3.
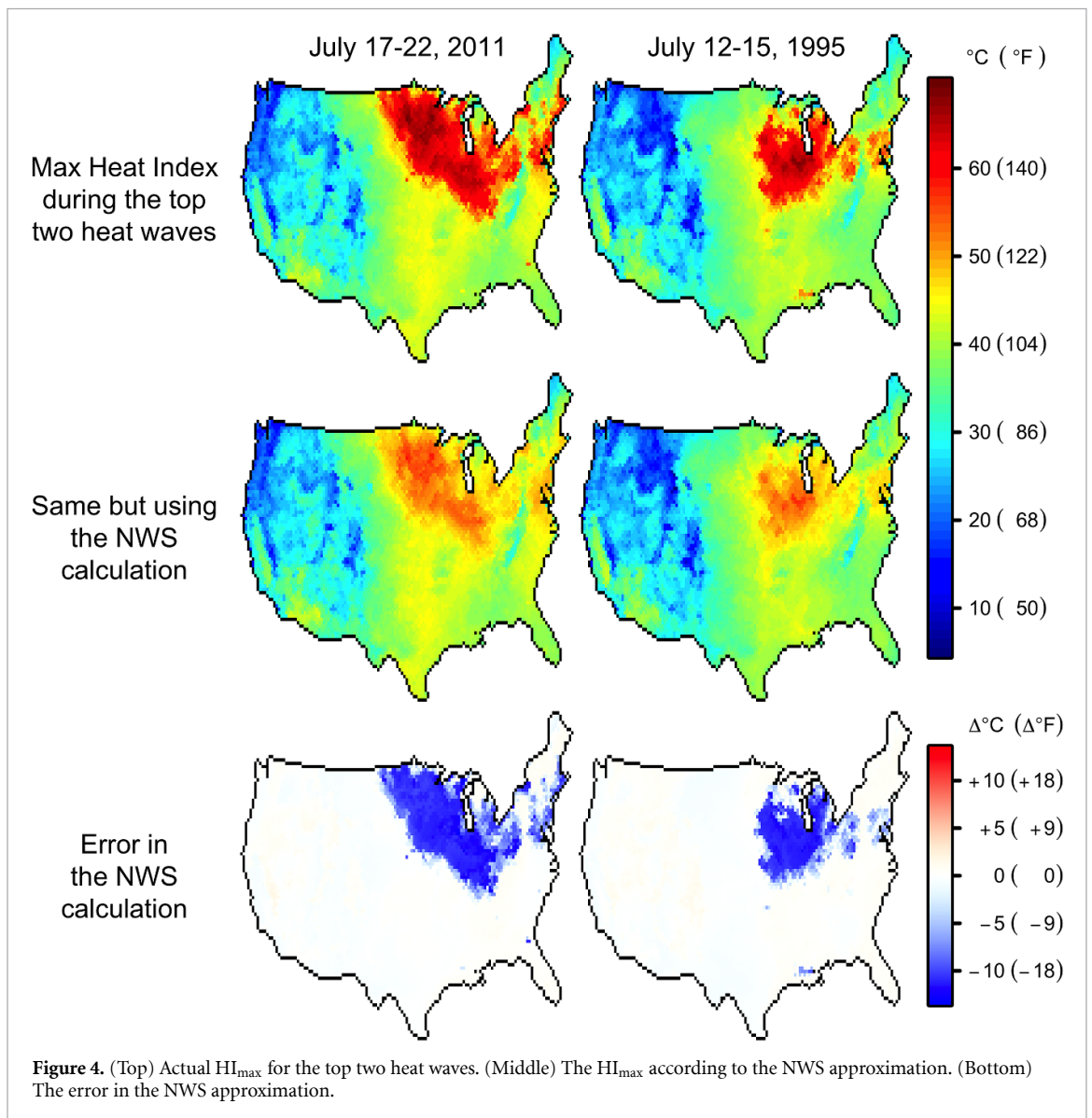
The top row of figure 4 displays HI_{max} during the top two heat waves. In both cases, the heat index reaches values well in excess of 60 °C (140 °F), reaching 70 °C (157 °F) during the 2011 heat wave and 68 °C (154 °F) during the 1995 heat wave. Compared to $HI_{max} - HI_{99.9}$, HI_{max} is more tightly peaked in the Midwest with typical values of ∼130 °F–150 °F.
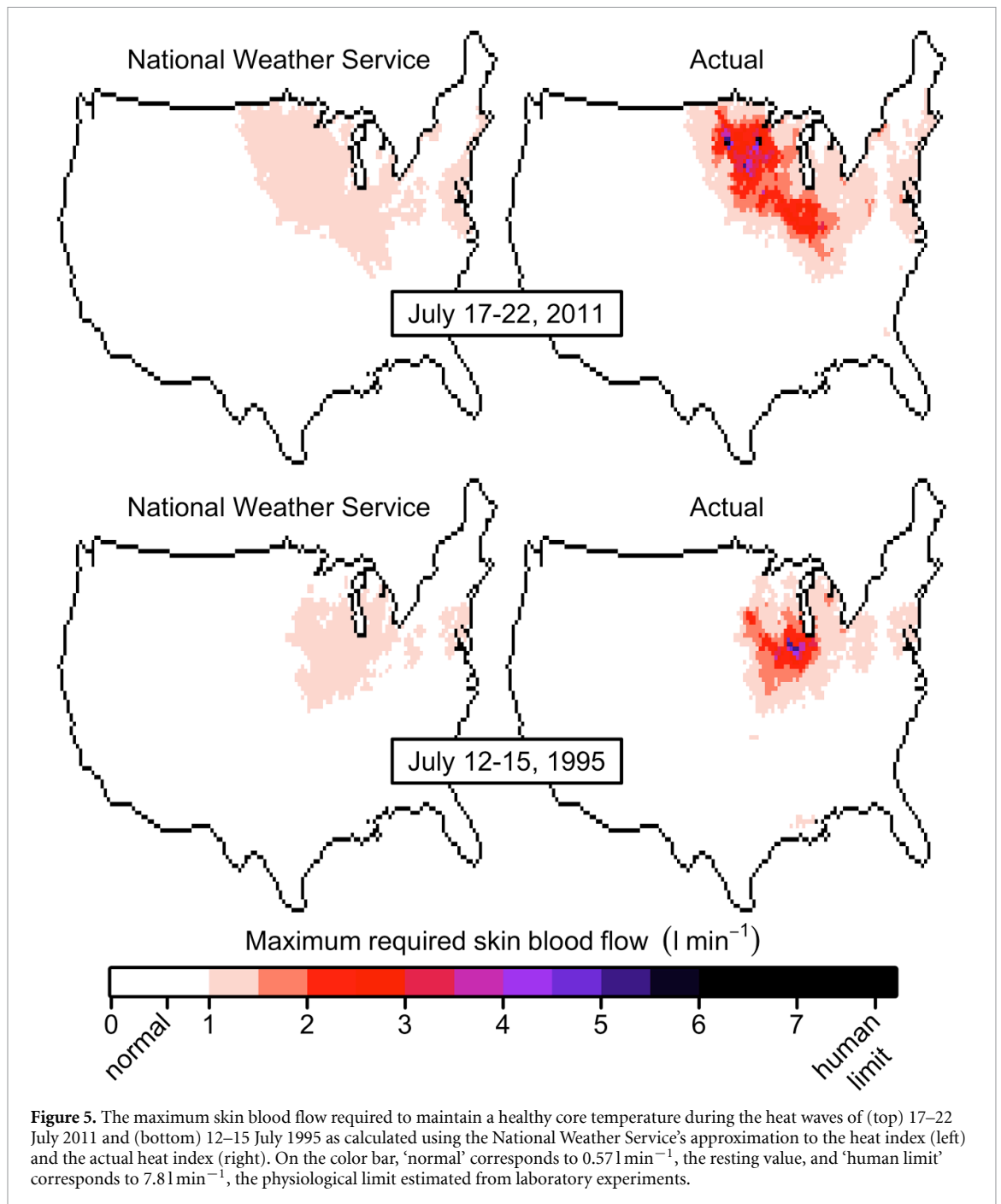
Since Steadman's original model fails for such high heat and humidity, the NWS has used its polynomial fit to report a heat index by extrapolation. The values resulting from that extrapolation are shown in the middle row of figure 4. The peak values of the heat index are noticeably muted in the NWS extrapolation. The error in the NWS extrapolation, shown in the bottom row of figure 4, is ∼10 °C (∼20 °F) for the peak values of the heat index.

During the July 1995 heat wave, the NWS reported a peak heat index of 119 °F at O'Hare airport and 125 °F at Midway airport. Those values were subsequently referenced by major newspapers (Kaye 1995, Lev and Ryan 1995, Nathans 1995, Stein and Kaplan 1995), the Centers for Disease Control and Prevention (1995), CDC, and research studies (Whitman *et al* 1997, Dematte *et al* 1998, Semenza *et al* 1999, Grady 2013). Using the

Table 1. Top 20 most severe CONUS heat waves from 1984 to 2020.

Rank	Dates	State with max HI	Max HI in °C (°F)	Max NWS value in °C (°F)
1	17–22 July 2011	North Dakota	70 (157)	59 (139)
2	12–15 July 1995	Illinois	68 (154)	57 (135)
3	31 July–4 August 2011	Mississippi	70 (158)	59 (139)
4	19–20 July 2019	Iowa	68 (155)	58 (136)
5	2–4 July 1997	Alabama	63 (145)	51 (124)
6	2–5 August 2010	Iowa	65 (149)	54 (129)
7	30 July 1999	Wisconsin	63 (146)	51 (124)
8	30 June–1 July 2011	Wisconsin	66 (150)	54 (129)
9	13–14 July 2010	Iowa	65 (149)	53 (127)
10	23–27 July 2005	Mississippi	61 (141)	50 (121)
11	10–11 July 2011	Indiana	64 (147)	52 (126)
12	1–3 July 2002	Maine	61 (141)	48 (119)
13	11–16 August 2010	Illinois	64 (147)	52 (126)
14	10–14 July 2002	Kentucky	47 (117)	43 (109)
15	01 July 2012	South Carolina	69 (155)	57 (135)
16	1–2 July 2020	Oklahoma	62 (144)	51 (125)
17	13–15 July 2015	Tennessee	65 (149)	52 (126)
18	12–14 August 2019	Louisiana	61 (143)	49 (120)
19	30 June–3 July 2018	Texas	59 (139)	46 (114)
20	30 July–3 August 2006	Illinois	62 (144)	51 (123)

Figure 4. (Top) Actual HI_{max} for the top two heat waves. (Middle) The HI_{max} according to the NWS approximation. (Bottom) The error in the NWS approximation.

Figure 5. The maximum skin blood flow required to maintain a healthy core temperature during the heat waves of (top) 17–22 July 2011 and (bottom) 12–15 July 1995 as calculated using the National Weather Service's approximation to the heat index (left) and the actual heat index (right). On the color bar, 'normal' corresponds to $0.57\,\mathrm{l\,min^{-1}}$, the resting value, and 'human limit' corresponds to $7.8\,\mathrm{l\,min^{-1}}$, the physiological limit estimated from laboratory experiments.

hourly temperature and relative humidity recorded at O'Hare and Midway, we find that the NWS extrapolation yields a peak HI of 118 °F at O'Hare airport at 1pm local time (when the temperature was 100 F and the relative humidity was 50%) and 124 °F at Midway airport at 12pm (temperature of 100 F and relative humidity of 55%), consistent with the reported values. Using these same temperature and humidity values, we can calculate the actual heat index to have been 123 °F at O'Hare (5 °F higher than reported by the NWS) and 141 °F at Midway (17 °F higher than reported by the NWS).

Like the original heat index, each value of the extended heat index maps one-to-one to thermoregulatory states (Lu and Romps 2022). For the extreme HI values in the Midwest during the July 2011 and July 1995 heat waves, a healthy adult walking in the shade would have been stressed physiologically in an effort to maintain a healthy core temperature: their body would need to sweat profusely (dripping sweat) and maintain a rapid rate of blood flow to the skin. This high blood flow would be needed to maintain an elevated skin temperature to ensure that the skin loses net energy to the environment at the same rate that metabolic heat is added to the core.

The right column of figure 5 shows the skin blood flow required to maintain a healthy core temperature at the times of the maximum heat index during the

top two heat waves. Combining the model of Steadman ([1979](#)) with the skin blood flow relation from Gagge *et al* ([1972](#)) (see Lu and Romps [2022](#)), the normal skin blood flow (i.e. in mild conditions) is $0.57\,\mathrm{l\,min^{-1}}$. Therefore, the dark red colors in figure 5 correspond to skin blood flows that are severalfold higher than usual, indicating a high state of physiological stress. The highest rate of skin blood flow measured in the laboratory, achieved by inducing severe thermal stress, is estimated to be around $7.8\,\mathrm{l\,min^{-1}}$ (Rowell [1974](#), Simmons *et al* [2011](#)). In the 2011 heat wave, there are a handful of grid cells of the reanalysis that report a required skin blood flow approaching $7.8\,\mathrm{l\,min^{-1}}$ and one grid cell that exceeds that value. In contrast, the required skin blood flow implied by the NWS approximation to the heat index, shown in the left column of figure 5, never exceeds $1.3\,\mathrm{l\,min^{-1}}$ during either heat wave.

5. Discussion

Using the heat index, which has recently been extended to high heat and humidity (Lu and Romps [2022](#)), the most physiologically stressful heat waves in the contiguous United States occur most often in the Midwest, not in the South as might be expected or previously reported (e.g. Smith *et al* [2013](#), Lyon and Barnston [2017](#)). The finding that the Midwest is home to the most hazardous heat and humidity is manifested both in the map of the 99.9th percentile of the daily maximum heat index $\mathrm{HI}_{99.9}$ (figure 2) and in the locations of the most severe heat waves as ranked by their exceedance of $\mathrm{HI}_{99.9}$ (figure 3). In both the July 1995 and July 2011 heat waves, the soils of the Midwest were moist when the high pressure arrived, trapping heat and humidity in a shallow boundary layer (Kunkel *et al* [1996](#), Moser [2011](#)). Although the ingredients of individual events can be described in this way, we are not aware of any first-principles theory for why the most severe US heat waves tend to occur preferentially in the Midwest.

The calculation used by the US National Weather Service underestimates the apparent temperature in extreme heat waves by as much as twenty degrees Fahrenheit. This has real consequences for our understanding of physiological impacts. For example, during the July 1995 heat wave, the heat index at the Midway airport hit a high of 141 °F. In other words, conditions in the shade at the airport felt the same as being in a room at 141 °F with 1.6 kPa of water-vapor pressure (8% relative humidity at that temperature). The physiological consequence of this exposure is that the cardiovascular system must maintain a skin blood flow that is elevated by 170%. In contrast, the heat index of 124 °F calculated by the NWS would imply a skin blood flow that is elevated by only 90%. As seen in the reanalysis, the discrepancy was even larger elsewhere in Illinois during the July 1995 heat wave, with the required skin blood flow elevated by 120%

according to the NWS approximation, but elevated by 820% according to the actual heat index. Thus, the approximate calculation used by the NWS, and widely adopted, inadvertently downplays the health risks of severe heat waves.

Conflict of interest

The authors declare no competing interests.

Appendix. The NWS approximation

The NWS approximation to the heat index is

$$\mathrm{HI} = \begin{cases} X & X \geqslant 80 \\ Y & X < 80 \end{cases}$$

with

$$
\begin{aligned}
X = &-42.379 + 2.04901523\,T + 10.14333127\,\mathrm{RH} \\
&- 0.22475541\,T\,\mathrm{RH} - 0.00683783\,T^2 \\
&- 0.05481717\,\mathrm{RH}^2 + 0.00122874\,T^2\,\mathrm{RH} \\
&+ 0.00085282\,T\,\mathrm{RH}^2 - 0.00000199\,T^2\,\mathrm{RH}^2 \\
&- \mathcal{H}(13 - \mathrm{RH})\mathcal{H}(T - 80)\mathcal{H}(112 - T) \\
&\times \frac{13 - \mathrm{RH}}{4}\sqrt{\frac{17 - |T - 95|}{17}} \\
&+ \mathcal{H}(\mathrm{RH} - 85)\mathcal{H}(T - 80)\mathcal{H}(87 - T) \\
&\times \frac{\mathrm{RH} - 85}{10}\frac{87 - T}{5} \\
Y = &\,0.5\Big[T + 61.0 + 1.2(T - 68.0) + 0.094\,\mathrm{RH}\Big],
\end{aligned}
$$

where $\mathcal{H}$ is the Heaviside unit step function and the variables T, RH, and HI in this expression are dimensionless: T is the temperature in degrees Fahrenheit, RH is the relative humidity in percent, and HI is the heat index in degrees Fahrenheit (Rothfusz [1990](#), National Weather Service [2014](#)). In the NWS implementation, HI is set equal to X or Y depending on whether X is greater than or less than 80. That leads to some very bad behavior at low temperatures. For example, at 0 °C (32 °F) and 70% relative humidity, the heat index would be given as 74 °C (166 °F). To avoid this problem, we modify the

NWS approximation to use $T = 80$ as the dividing line between these two expressions:

$$\text{HI} = \begin{cases} X & T \geqslant 80 \\ Y & T < 80 \end{cases}.$$

This eliminates the poor behavior at cooler temperatures and does not affect the performance of the approximation at warmer temperatures.

ORCID iD

David M Romps ⬤ https://orcid.org/0000-0001-7649-5175

References

Acharya P, Boggess B and Zhang K 2018 Assessing heat stress and health among construction workers in a changing climate: a review *Int. J. Environ. Res. Public Health* **15** 247

Amnuaylojaroen T, Limsakul A, Kirtsaeng S, Parasin N and Surapipith V 2022 Effect of the near-future climate change under RCP8.5 on the heat stress and associated work performance in Thailand *Atmosphere* **13** 325

Anderson G B, Bell M L and Peng R D 2013 Methods to calculate the heat index as an exposure metric in environmental health research *Environ. Health Perspect.* **121** 1111–9

Berry M, Fagliano J, Tsai S, McGreevy K, Walsh A and Hamby T 2013 Evaluation of heat-related illness surveillance based on chief complaint data from New Jersey hospital emergency rooms *Online J. Public Health Inform.* **5** e125

Carleton T A *et al* 2020 Valuing the global mortality consequences of climate change accounting for adaptation costs and benefits *Technical Report* (National Bureau of Economic Research)

Centers for Disease Control and Prevention 1995 Heat-related mortality—Chicago, July 1995 *Morb. Mortal. Wkly. Rep.* **44** 577–9

Changnon S A, Kunkel K E and Reinke B C 1996 Impacts and responses to the 1995 heat wave: a call to action *Bull. Am. Meteorol. Soc.* **77** 1497–506

Dahl K, Licker R, Abatzoglou J T and Declet-Barreto J 2019 Increased frequency of and population exposure to extreme heat index days in the United States during the 21st century *Environ. Res. Commun.* **1** 075002

Delworth T L, Mahlman J D and Knutson T R 1999 Changes in heat index associated with CO_2-induced global warming *Clim. Change* **43** 369–86

Dematte J E, O'Mara K, Buescher J, Whitney C G, Forsythe S, McNamee T, Adiga R B and Ndukwu I M 1998 Near-fatal heat stroke during the 1995 heat wave in Chicago *Ann. Intern. Med.* **129** 173–81

Diem J E, Stauber C E and Rothenberg R 2017 Heat in the southeastern United States: characteristics, trends and potential health impact *PLoS One* **12** e0177937

Diffenbaugh N S, Pal J S, Giorgi F and Gao X 2007 Heat stress intensification in the Mediterranean climate change hotspot *Geophys. Res. Lett.* **34** L11706

Dosio A, Mentaschi L, Fischer E M and Wyser K 2018 Extreme heat waves under 1.5 °C and 2 °C global warming *Environ. Res. Lett.* **13** 054006

Fuhrmann C M, Sugg M M, Konrad C E and Waller A 2016 Impact of extreme heat events on emergency department visits in North Carolina (2007–2011) *J. Commun. Health* **41** 146–56

Gagge A P, Stolwijk J A J and Nishi Y 1972 An effective temperature scale based on a simple model of human physiological regulatory response *ASHRAE Trans.* **7** 247–62

Grady S C 2013 Climate change vulnerability and impacts on human health *Climate Change in the Midwest: Impacts, Risks, Vulnerability and Adaptation* ed S C Pryor (Bloomington, IN: Indiana University Press) ch 9, pp 117–33

Kaye H 1995 Mayor, utility—both fail as heat kills hundreds *People's Weekly World (1990–2013)* 9

Kim H, Ha J-S and Park J 2006 High temperature, heat index and mortality in 6 major cities in South Korea *Arch. Environ. Occup. Health* **61** 265–70

Kunkel K E, Changnon S A, Reinke B C and Arritt R W 1996 The July 1995 heat wave in the Midwest a climatic perspective and critical weather factors *Bull. Am. Meteorol. Soc.* **77** 1507–18

Lev M and Ryan N 1995 City sweats, but survives: emergency effort, breezes combine to fend off disaster *Chicago Tribune (1963–1996)* p 2

Lu Y-C and Romps D M 2022 Extending the heat index *J. Appl. Meteorol. Climatol.* accepted (https://doi.org/10.1175/JAMC-D-22-0021.1)

Lyon B and Barnston A G 2017 Diverse characteristics of US summer heat waves *J. Clim.* **30** 7827–45

Meehl G A and Tebaldi C 2004 More intense, more frequent and longer lasting heat waves in the 21st century *Science* **305** 994–7

Mesinger F *et al* 2006 North American regional reanalysis *Bull. Am. Meteorol. Soc.* **87** 343–60

Modarres R, Ghadami M, Naderi S and Naderi M 2018 Future heat stress arising from climate change on Iran's population health *Int. J. Biometeorol.* **62** 1275–81

Moser W 2011 Chicago heat wave: blame this spring's floods *Chicago Magazine*

Nathans A 1995 City heat index soars to 119; relief in sight *Indianapolis Star (1923–2004)* 1

National Weather Service 2014 The heat index equation (available at: www.wpc.ncep.noaa.gov/html/heatindex_equation.shtml) (Accessed 16 February 2022)

O'Neill M S, Zanobetti A and Schwartz J 2005 Disparities by race in heat-related mortality in four US cities: the role of air conditioning prevalence *J. Urban Health* **82** 191–7

Opitz-Stapleton S, Sabbag L, Hawley K, Tran P, Hoang L and Nguyen P H 2016 Heat index trends and climate change implications for occupational heat exposure in Da Nang, Vietnam *Clim. Serv.* **2–3** 41–51

Perera T A N T, Nayanajith T M D, Jayasinghe G Y and Premasiri H D S 2022 Identification of thermal hotspots through heat index determination and urban heat island mitigation using ENVImet numerical micro climate model *Model. Earth Syst. Environ.* **8** 209–26

Rahman M B, Salam R, Reza A, Islam M T, Tasnuva A, Haque U, Shahid S, Hu Z and Mallick J 2021 Appraising the historical and projected spatiotemporal changes in the heat index in Bangladesh *Theor. Appl. Climatol.* **146** 125–38

Rao K K, Kumar T V L, Kulkarni A, Ho C H, Mahendranath B, Desamsetti S, Patwardhan S, Dandi A R, Barbosa H and Sabade S 2020 Projections of heat stress and associated work performance over India in response to global warming *Sci. Rep.* **10** 16675

Robinson P J 2001 On the definition of a heat wave *J. Appl. Meteorol. Climatol.* **40** 762–75

Rothfusz L P 1990 The heat index "equation" (or, more than you ever wanted to know about heat index) *Technical Attachment* SR 90-23 (Forth Worth, TX: NWS Southern Region Headquarters)

Rowell L B 1974 Human cardiovascular adjustments to exercise and thermal stress *Physiol. Rev.* **54** 75–159

Semenza J C, McCullough J E, Flanders W D, McGeehin M A and Lumpkin J R 1999 Excess hospital admissions during the July 1995 heat wave in Chicago *Am. J. Prev. Med.* **16** 269–77

Semenza J C, Rubin C H, Falter K H, Selanikio J D, Flanders W D, Howe H L and Wilhelm J L 1996 Heat-related deaths during the July 1995 heat wave in Chicago *New Engl. J. Med.* **335** 84–90

Simmons G H, Wong B J, Holowatz L A and Kenney W L 2011 Changes in the control of skin blood flow with exercise training: where do cutaneous vascular adaptations fit in? *Exp. Physiol.* **96** 822–8

Smith T T, Zaitchik B F and Gohlke J M 2013 Heat waves in the United States: definitions, patterns and trends *Clim. Change* **118** 811–25

Steadman R G 1979 The assessment of sultriness. Part I: a temperature-humidity index based on human physiology and clothing science *J. Appl. Meteorol.* **18** 861–73

Stein S and Kaplan J 1995 Scientists probe why heat wave became a killer *Chicago Tribune (1963–1996)* 2

Storm B and Fowler B 2011 Evaluating the relationship between heat-related ED visits and weather variables *Emerg. Health Threats J.* **4** 146

Tustin A W, Lamson G E, Jacklitsch B L, Thomas R J, Arbury S B, Cannon D L, Gonzales R G and Hodgson M J 2018 Evaluation of occupational exposure limits for heat stress in outdoor workers—United States, 2011–2016 *Morb. Mortal. Wkly. Rep.* **67** 733

Whitman S, Good G, Donoghue E R, Benbow N, Shou W and Mou S 1997 Mortality in Chicago attributed to the July 1995 heat wave *Am. J. Public Health* **87** 1515–8

Xie J, Chen Y, Hong T and Laing T D 2018 Relative humidity for load forecasting models *IEEE Trans. Smart Grid* **9** 191–8

Xu Z, FitzGerald G, Guo Y, Jalaludin B and Tong S 2016 Impact of heatwave on mortality under different heatwave definitions: a systematic review and meta-analysis *Environ. Int.* **89** 193–203

Yip F Y, Flanders W D, Wolkin A, Engelthaler D, Humble W, Neri A, Lewis L, Backer L and Rubin C 2008 The impact of excess heat events in Maricopa County, Arizona: 2000–2005 *Int. J. Biometeorol.* **52** 765–72